Development of chemiluminescent lab-on-fiber immunosensor for rapid point-of-care testing of anti-SARS-CoV-2 antibodies and evaluation of longitudinal immune response kinetics following three-dose inactivation virus vaccination

Wenjuan Xu[a,§], Dan Song[a,§], Jiayao Liu[a], Xiangzhi Han[a], Jiaxin Xu[a], Anna Zhu[b,*], Feng Long[a,c*]

[a] *School of Environment and Natural Resources, Renmin University of China, Beijing, 100872, China*

[b] *State Key Laboratory of NBC Protection for Civilian, Beijing, 102205, China*

[c] *Department of Chemistry, Renmin University of China, Beijing, 100872, China*

* Corresponding author: chuanna0306@163.com; longf04@ruc.edu.cn

[§] These authors have equal contribution for this work.

Abstract：Developing reliable, rapid, and quantitative point-of-care testing (POCT) technology of SARS-CoV-2 specific antibodies and understanding longitudinal vaccination response kinetics are highly required to restrain the ongoing Coronavirus Disease 2019 (COVID-19) pandemic. We demonstrate a novel portable, sensitive, and rapid chemiluminescent lab-on-fiber detection platform for detection of anti-SARS-CoV-2 antibodies: the c-LOFI. Using

This is the author manuscript accepted for publication and undergone full peer review but has not been through the copyediting, typesetting, pagination and proofreading process, which may lead to differences between this version and the Version of Record. Please cite this article as doi: 10.1002/jmv.28190.

SARS-CoV-2 Spike S1 RBD protein functionalized fiber bio-probe, the c-LOFI can detect anti-SARS-CoV-2 IgG and IgM antibodies with high sensitivity based on their respective HRP labeled secondary antibodies. The limits of detection of anti-SARS-CoV-2 IgG and IgM antibodies were 0.6 ng/ mL and 0.3 ng/mL, respectively. The c-LOFI was successfully applied for direct detection of anti-SARS-CoV-2 antibodies in whole blood samples with simple dilution, which can serve as a finger prick test to rapidly detect antibodies. Furthermore, the longitudinal immune response (>12 months) kinetics following three-dose inactivated virus vaccines was evaluated based on anti-SARS-CoV-2 IgG detection results, which can provide importance significance for understanding the immune mechanism against COVID-19 and identify individuals who may benefit from the vaccination and booster vaccination. The c-LOFI has great potential to become a sensitive, low-cost, rapid, high-frequency POCT tool for the detection of both SARS-CoV-2 specific antibodies and other biomarkers.

Graphic abstract

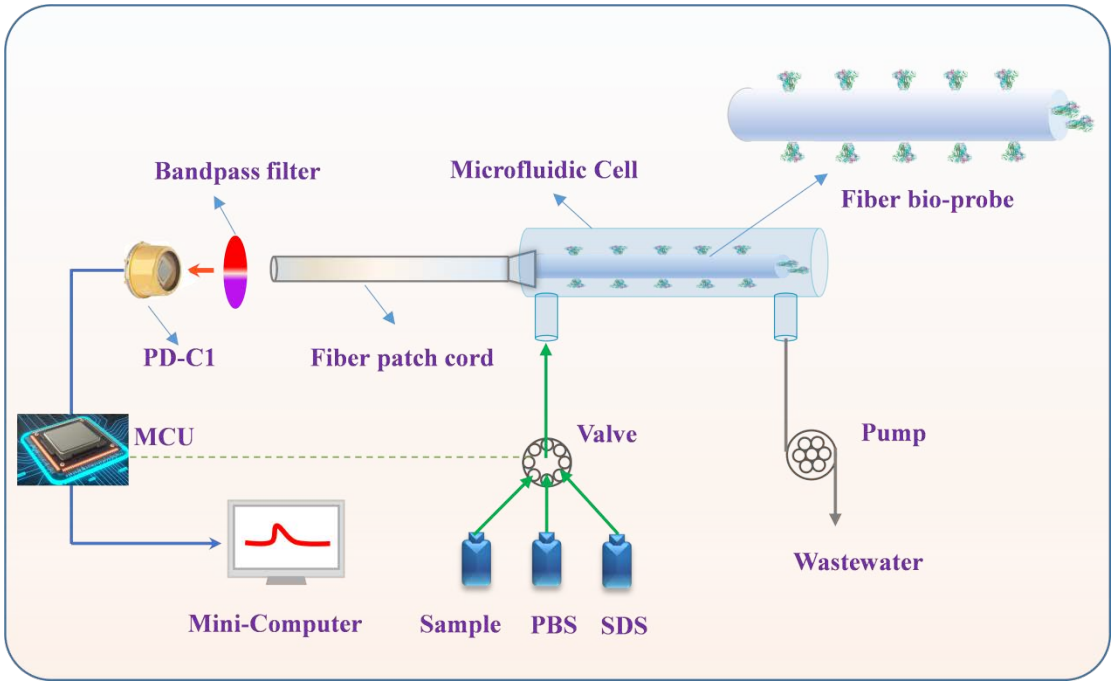

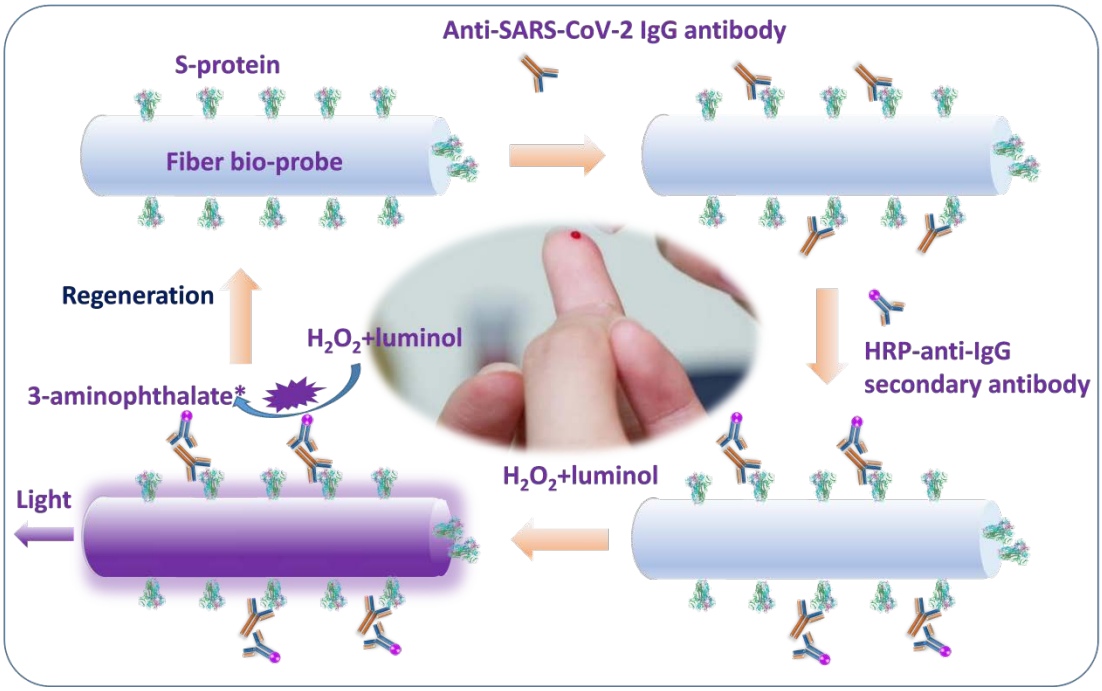

Keywords: Lab-on-fiber immunosensor; Anti-SARS-CoV-2 antibody; Chemiluminescent immunoassay; Immune response kinetics; Vaccination

1. Introduction

Since 2019, worldwide experienced unprecedented morbidity and mortality because of the Coronavirus Disease 2019 (COVID-19) pandemic that caused by the severe acute respiratory syndrome coronavirus 2 (SARS-CoV-2) [1-4]. To restrain the spread of COVID-19, many vaccines in the world have obtained emergency use certification [5]. The objective of vaccination is to induce anti-SARS-CoV-2 antibodies to reduce infection and form a population immune barrier [6-8]. Quantitative measurement of specific antibody is essential for assessing the immune acquisition and long-term protection effect after vaccination and improving vaccination deployment based on the herd immunity level. Particularly, more and more virus mutants have been reported which have stronger transmissibility and pathogenicity [9,10]. To better guide the early treatment of patients, investigate asymptomatic infection, promote the research and

development of new mutant virus vaccine, understanding individual immunity to SARS-CoV-2 is the basis and premise of research [2,11,12].

Anti-SARS-CoV-2 antibodies tests, especially point-of-care testing (POCT) in whole blood, is very important for rapid and convenient evaluation of human immunity [4,8,13]. Commercial testing kits, including lateral flow immunochromatographic assay (LFIA) [14,15], enzyme-linked immune sorbent assay (ELISA) [16], and chemiluminescence enzyme immunoassay (CLIA) [17,18], have been available for the anti-SARS-CoV-2 antibodies detection. LFIA is simple and rapid on-site detection technology, but it is primarily used as binary qualitative tests with a low sensitivity [19,20]. ELISA has widely been used for the evaluation of vaccination effect with high accuracy and sensitivity [16]. With the advantages of high sensitivity, high degree of automation and low detection risk, CLIA has important clinical significance in SARS-CoV-2 IgM/lgG antibodies detection [18,21]. However, most of these methods only measure antibody titer, which is qualitative and difficult to compare with those results due to the use of different testing kits. Moreover, they require a centralized laboratory for diagnostics because of the requirement of expensive and bulky instrument, complex separation and washing steps, long assay time, and trained professional, which make them be difficult for POCT [4,13]. In line with this, developing novel reliable quantitative POCT technology of anti-SARS-CoV-2 antibodies are highly needed to deal with the current massive attack.

In this study, a simple and rapid chemiluminescent lab-on-fiber immunosensor (c-LOFI) was at the first time built to meet the increasing needs for a wide range of antibody detection facing up to the ongoing pandemic and the deployment of whole population vaccination. Lab-on-fiber (LOF) technology has attracted great attention because its unprecedented features such as

miniaturization, functionalities and integration, which is intriguing in biosensing research field [22,23]. The ideal LOF integrating functional materials and components with micro/nano scale, so as to realize the transformation from optical fiber to multifunctional sensor [24]. In our system, a functional fiber bio-probe was used as a biorecognition and separated element as well as a transducer. This bio-probe replaces immuno-magnetic-beads in traditional CL biosensors to capture, concentrate, and separate targets, which significantly simplify the assay steps and increases the collection efficiency of CL and the sensitivity. Understanding antibody response kinetics for vaccines is crucial for the rational design, long-term protect efficacy, vaccine program and for evaluating the trend of COVID-19 epidemic in the future. Using c-LOFI, we investigated the immune response kinetics over time following three-dose inactivated virus vaccines for up to 12 months based on the proposed anti-SARS-CoV-2 IgG detection method.

2. Experimental

2.1 Reagents and chemicals

See Supporting Information (Section 1) for reagents and chemicals used in this work.

2.2 Functionalization of bio-probe for anti-SARS-CoV-2 IgM/IgG antibody detection

The S-protein was immobilized on the fiber bio-probe for the detection of anti-SARS-CoV-2 IgG and IgM antibody (IgG-S and IgM-S) detection according to previous method with minor modification (Details in Supporting Information and Fig.S1).

2.3 Design of the c-LOFI and its application for antibody detection

Scheme 1A show the schematic of the c-LOFI, consisting of microfluidic system, optical system, signal treatment and control system, and mini-computer. The photo of the c-LOFI was showed in Fig.S2. Optical system, including fiber bio-probe, fiber patch cord, and photodetector, is the key section of the entire sensor because it determines the sensitivity, portability, and stability. In the c-LOFI, the S-protein functionalized fiber bio-probe is employed not only as biorecognition element, but also as separated element and transducer. The chemiluminescence is collected by the bio-probe and detected by PD-C1 detector after transmission of fiber patch cord and filtering using bandpass filter. In the microfluidic system, the peristaltic pump and six-way injection valve are used for sequentially introducing various fluids into the metal cylindrical microfluidic cell. The fiber bio-probe is embedded in the microfluidic cell (ϕ 0.8 × 30.0 mm) with an effective volume of 15.0 μL. Signal treatment and control system is built based on a microcontroller unit (MCU), which is used for the treatment of the chemiluminescence signal and controlling the pump and valve operation. The dynamic detection curve and final detection result are shown in display screen.

Taking IgG-S for example, the quantitative detection of the anti-SARS-CoV-2 antibodies is achieved based on the sandwich chemiluminescent immunoassay principle (Scheme 1B). First, S-protein functionalized bio-probe is placed in the microfluidic cell, and 15.0 μL of sample containing various concentration of IgG-S is introduced in it for a certain time. In this phase, IgG-S specifically bind with S-protein on the surface of fiber bio-probe. Second, after PBS buffer is pumped to the cell to remove free IgG-S, a certain concentration of the HRP labeled anti-IgG secondary antibodies is added into the cell, and part of them bind with the IgG-S. Third, after washing the free secondary antibodies using PBS

buffer, 15.0 μL CL substrate solution is pumped into the surface of fiber bio-probe where the CL intensity is real-time detected from the HRP -catalyzed luminescence of substrates. The detectable CL intensity is related with the concentration of IgG-S, which is used for their quantitative detection. Finally, the bio-probe is regenerated for 300 s with SDS solution (0.5%, pH 1.9) and rinsed with PBS buffer to reuse. The whole process of detection is less than 30 min.

3. Results and discussion

3.1. Characterization of S-protein functionalized bio-probe and c-LOFI

To evaluate the c-LOFI performance, the S-protein functionalized bio-probe was placed in microfluidic cell for immunoassay of IgG-S/IgM-S. First, IgG-S was detected using c-LOFI, and Fig. 1A shows the typical signal curve of IgG-S detection. 15.0 μL IgG-S of 5.0 μg/mL was introduced into the microfluidic cell for 300 s incubation reaction, and part of them bound with the S-protein immobilized on the fiber surface. After washing with PBS, 15.0 μL HRP labeled secondary antibodies of 0.5 μg/mL was then delivered to the microfluidic cell. Some of the secondary antibodies reacted with IgG-S for 400 s. After the excess secondary antibodies washed away using PBS, 15.0 μL CL substrate solution was introduced to perform the CL detection. From Fig. 1A, an abruptly increasing chemiluminescence signal was detected by the PD-C1 detector after addition of the CL substrate solution due to the HRP catalysis. The CL signal (I_s) for detection is calculated as the difference of the CL intensity at the peak (I_p) and the baseline (I_b).

$$I_s=I_p-I_b \quad (1)$$

Second, IgM-S was also determined based on similar immunoassay principle (Fig. 1B). 15.0 μL IgM-S of 100 ng/mL was primarily pumped over the S-protein

functionalized bio-probe for incubation reaction. After washing, HRP labeled anti-IgM secondary antibody was added to bind with IgM-S bound on the bio-probe surface. Then, CL substrate solution was added to perform the CL detection. The same as the IgG-S detection, the CL signal also increased after the addition CL substrate solution (Fig. 1B).

Third, to further verify the CL signal generated from the immunoassay reaction, several control experiments were performed (Fig. 1C). (a) The CL substrate solution was directly delivered in the microfluidic cell, and no CL signal was detected. (b) and (c) The HRP labeled anti-IgG secondary antibody or HRP labeled anti-IgM secondary antibody was initially added for incubation, and the CL substrate solution was then delivered. A low CL signal was detected, which originated from the non-specific adsorption of secondary antibody. (d) The IgM-S, HRP labeled anti-IgG secondary antibody, and the CL substrate solution were sequentially introduced. The CL signal could also be detected due to the non-specifical adsorption of HRP labeled anti-IgG secondary antibody, but it was significantly lower than that using HRP labeled anti-IgM secondary antibody. (e) The IgG-S, HRP labeled anti-IgM secondary antibody, and the CL substrate solution were sequentially introduced. Similarly, a lower CL signal was obtained compared with that using HRP labeled anti-IgG secondary antibody. For comparison, the functionalized fiber bio-probe were also characterized using the confocal fluorescence microscope (Nikon A1, Japan, 638 nm). From Fig. 1D-a, no fluorescence is observed on the surface of S-protein modified bio-probe. A little fluorescence is demonstrated after Cy5.5-labeled secondary antibody is pumped over the bio-probe (Fig. 1D-b), which contributes to non-specific adsorption. However, when IgG-S and Cy5.5-labeled secondary antibody was sequentially introduced, a clear fluorescence image was obtained (Fig. 1D-c). The above results demonstrated that the S-protein was successfully immobilized on the

bio-probe. The detected CL signal mainly originated from the specifical binding of S-protein, IgG-S, and anti-IgG secondary antibody, or S-protein, IgM-S, and anti-IgM secondary antibody. Although both IgG-S and IgM-S could specifically bind with S-protein, they might bind with the different section of S-protein and did not affect each other. Therefore, using the S-protein modified fiber bio-probe, either IgG-S or IgM-S could be detected just using HRP-anti-IgG secondary antibody or HRP-anti-IgM secondary antibody, respectively.

To further verify specificity of the S-protein functionalized fiber bio-probe, other three antibodies (anti-MERS-CoV antibody, anti-HCoV-HKU1 antibody, and normal Human IgG) were tested. From Fig. 1E, the individual addition of three antibodies does not induce the increase of CL, which is similar to that of blank sample. However, the mixture of anti-MERS-CoV, anti-HCoV-HKU1, normal Human IgG, and IgM-S antibody was introduced into the optofluidic cell, a significant CL intensity was obtained, which is almost identical to that of IgM-S antibody. Therefore, the proposed method was highly specific for IgM-S and IgG-S detection, which depended on high specificity of IgM-S and IgG-S to S-protein and the secondary antibodies to IgG-S or IgM-S.

Finally, the reusability of the S-protein functionalized fiber bio-probe was also investigated. From Fig. 1 and Fig.S3, when the regeneration solution was pumped over the cell, the signal curve return to the baseline. In this process, all the bound antibodies were dissociated from the surface of the optical fiber. After washing by PBS buffer, a similar CL signal was again detected when the IgG-S/IgM-S, and HRP-anti-IgG/IgM secondary antibody were sequentially added (Fig.S3A and B). The experimental result show that the functional bio-probe could be reused more than 15 times without obvious detection performance loss (Fig.S3C and D). The reusability of bio-probe not only saves

detection cost, but also increases the accuracy of detection results. All these results show that the proposed c-LOFI can provide a good solution for the quantitative detection of IgG-S/IgM-S based on the sandwich immunoassay mechanism.

3.2 Detection parameter optimalization

Several parameters, including SARS-CoV-2 S-protein concentration, the incubation time of primary antibody, the concentration and incubation time of HRP-labeled secondary antibody, were optimized. The concentration of S protein covalently attached on the fiber surface is a key factor to affect the signal output. S-protein of various concentrations ranging from 0.05 to 0.5 mg/mL were applied for the functionalization of bio-fiber probe (Supporting information). Figure S4A and S4B shows that the CL intensity increases with increasing the concentration of S protein and reaches a plateau for the detection of both IgM-S and IgG-S. The optimal concentration of S-protein was 0.3 mg/mL considering the CL intensity and the reagent consumption.

To determine the optimal incubation time between IgG-S/IgM-S and S-protein immobilized onto the bio-probe surface, the incubation time ranging from 0 to 9 min was tested. Fig.S4C and S4D shows that the CL intensity increased rapidly over time when the incubation time of IgM-S and IgG-S was less than 5 min and 3 min, respectively, and then reached a plateau, which was used as the optimal time. The secondary antibody reaction time was optimized. Fig.S4E and S4F displayed that the CL signal increased obviously when the reaction time of anti-IgM and IgG secondary antibodies was less than 7 min and remained basically the same over time. Thus, the optimal time was set at 7 min.

The concentration of HRP labeled secondary antibody is one of key factors for the detection of IgG-S/IgM-S. To study the optimum secondary antibody concentration, a sensitivity index (ε) was defined as follows.

$$\varepsilon = \frac{I_S - I_0}{I_S} \quad (2)$$

where I_0 and I_s are the CL intensities of the sandwich chemiluminescent immunoassay without or with primary antibody (IgG-S/IgM-S), respectively. In practical use, the best secondary antibody concentration was determined considering several criteria. First, the stronger CL intensity should be obtained in the present of IgG-S or IgM-S. Second, higher ε should be achieved (**>** 0.60) to improve detection sensitivity. Fig.S4H and S4G shows the CL intensities without or with primary antibody significantly increased with increasing secondary antibody concentration for both IgG-S and IgM-S, respectively. The maximum ε for IgG-S and IgM-S were 0.62 and 0.67 when secondary antibodies were 0.5 μg/mL and 1.0 μg/mL, respectively, which were used as optimum condition for subsequent IgG-S and IgM-S measurements.

3.3 Dose-response curve of anti-SARS-CoV-2 IgM/IgG antibody in PBS

Once optimizing detection parameters, quantification analysis of IgM-S/IgG-S was done based on sandwich chemiluminescent immunoassay principle. The typical CL signal traces for IgM-S/IgG-S detection was shown in Fig. 2A and 2B, respectively, which illustrated increasing concentration of both IgM-S and IgG-S led to proportional enhancement of their CL intensities. To obtain the dose-response curves, the normalization value of a certain IgM-S or IgG-S, N_{IgM} and N_{IgG}, is calculated as following.

$$N_{\mathrm{IgM}} = \frac{I_{\mathrm{s,IgM}} - I_{\mathrm{b,IgM}}}{I_{\mathrm{s,IgM,max}} - I_{\mathrm{b,IgM}}} \quad (3)$$

$$N_{\mathrm{IgG}} = \frac{I_{\mathrm{s,IgG}} - I_{\mathrm{b,IgG}}}{I_{\mathrm{s,IgG,max}} - I_{\mathrm{b,IgG}}} \quad (4)$$

where $I_{\mathrm{s,IgM,max}}$ and $I_{\mathrm{s,IgG,max}}$ are the CL intensities at the maximum IgM-S or IgG-S concentration, respectively; $I_{\mathrm{b,IgM}}$ and $I_{\mathrm{b,IgG}}$ are the CL intensities of the blank samples without IgM-S or IgG-S, respectively; $I_{\mathrm{s,IgM}}$ and $I_{\mathrm{s,IgG}}$ are the CL intensities of the samples with different antibody concentrations.

The dose-response curves for IgM-S and IgG-S were plotted against the concentration logarithm using a four-parameter logistic equation, respectively (Fig. 2C and Fig. 2D). The error bars shown in the Fig. 2C and 2D are less than 10%, indicating the excellent stability of the proposed methods. The limit of detection (LODs) of IgM-S and IgG-S is 0.3 ng/mL and 0.4 ng/mL using three times standard deviation of the mean blank values, respectively. These LODs is lower than those of ELISA (4.2 ng/mL and 0.6 ng/mL for IgM-S and IgG-S, respectively, shown in Fig.S5), Considering between 20% and 80% of inhibition, the linear response of IgM-S and IgG-S ranged from 0.5 ng/mL to 19.1 ng/mL and from 2.1 ng/mL to 1084.5 ng/mL, respectively. Table S1 presents the biosensing features of our platform and other previous works, including the targets and LODs.

3.4 Detection of anti-SARS-CoV-2 IgG/IgM antibody in blood

Direct on-site detection of IgM-S and IgG-S antibodies in whole blood greatly benefits for rapid diagnosis and appropriate treatment of COVID-19 patients [25,26]. Unfortunately, the complexities of whole blood, containing many organic components including proteins, amino acids, or lipids, are challenging for their immunoassay due to the matrix effect on immunoassay [27,28]. Herein, we explored the matrix effect of whole blood on detection of IgG-S or IgM-S. The IgG-S or IgM-S was spiked into PBS, primary whole blood, 5, 10, 20, and 30

times diluted blood, respectively, with a final concentration of 50.0 ng/mL. These samples were detected by the proposed method. Fig.S6 demonstrates that the CL intensity of primary whole blood is quite lower than that of PBS, which resulted from the inhibition of the blood matrix on the antibody-antigen interaction. With increasing the dilution times, the detectable CL intensity increased, and was similar that in PBS when the whole blood was diluted more than 20 times, suggesting that the dilution blood could be directly used for IgG-S and IgM-S detection. The common methods to eliminate blood matrix effects, such as sample extraction and cleanup procedures, are generally time-consuming, laborious, and not suitable for POCT [29-31]. Dilution of the blood sample is a simple and useful method to achieve on-site POCT detection. Therefore, blood samples diluted 20 times were used in subsequent experiments.

After confirming the capability of c-LOFI to detect antibody in whole blood, standard curves were established to measure IgG-S and IgM-S using healthy donors' blood without vaccination. After spiked with various amount of IgG-S and IgM-S, the whole blood samples were detected using c-LOFI. Similar with those in PBS, increasing concentration of both IgG-S and IgM-S also resulted in proportional enhancement of their CL intensities. The dose-response curves for IgM-S and IgG-S were plotted against the logarithm of their concentrations (Fig. 3A and 3B). The LODs of IgM-S and IgG-S is 0.3 ng/mL and 0.6 ng/mL, respectively, which are similar with those in PBS. Considering between 20% and 80% of inhibition, the linear response of IgM-S and IgG-S ranged from 0.6 ng/mL to 23.7 ng/mL and from 1.8 ng/mL to 984.9 ng/mL, respectively (Fig. 3C and 3D).

To further prove the feasibility of our device in the real scenario, we applied the c-LOFI to quantify IgG in negative finger blood samples and positive finger blood samples with vaccine. In five negative finger blood samples, no IgG-S was

detected because they did not either vaccine or infect the SARS-CoV-2 virus. Then, these samples were spiked with various concentrations of IgG-S and IgM-S detected using the c-LOFI. Table S2 and Table S3 shows that the recovery rates of the spiked samples are in the range of 77%-136% with relative standard derivations of less than 10%. Furthermore, the IgG-S originated from five vaccination volunteers finger blood samples were also detected using the c-LOFI. The concentrations of IgG-S was from 17.1 to 182.1 ng/mL, which were consistent with those detected by ELISA (Table S4). These results demonstrated that the c-LOFI system can be regarded as a reliable method of quantitative analysis of IgG-S and IgM-S. More importantly, the c-LOFI can directly be applied for the rapid detection of the whole blood sample, which is especially useful for on-site patient diagnosis.

Compared with various reported POCT devices [32], c-LOFI has outstanding advantages in high sensitivity and quantitative analysis. First, the c-LOFI has low background signal and high signal-to-noise ratio, which allows a high sensitivity. Second, the specific recognition sites of IgM-S/IgG-S can be increased by modifying the number of the biorecognition molecules on the surface of bio-probe, which can decrease the amount of IgM-S/IgG-S to obtain the same CL intensity. Third, the S-protein immobilized on the surface by chemical modification keep high activity toward IgM-S/IgG-S to reduce the non-specific adsorption. In additional, the c-LOFI has other superiority, such as easy-to-use, portability, cost-effectiveness, and rapidity.

3.5 Immune kinetics with three-dose inactivation virus vaccination

Anti-SARS-CoV-2 humoral response kinetics benefits for COVID-19 diagnosis and vaccine development. Lacking protective immunity may induced by decreasing antibody levels [33]. Many vaccines have officially approved for

emergence use including inactivated virus vaccines, RNA/DNA vaccines, and subunit vaccines. Among them, inactivated virus vaccines are one of the most promising choices because they retain all of the antigenic components of the corresponding virus and have several significant features, such as potentially high efficacy, low cost, high feasibility, and high safety. The IgG is the most robust and durable antibody against the SARS-CoV-2 virus after vaccine and infection. Therefore, evaluating anti-SARS-CoV-2 IgG antibodies level is pivotal to monitor the immune response. Studies have reported that IgG could persist for 3 to 8 months in human body after SARS-CoV-2 infection symptom [34,35]. However, IgG antibodies with longer-term kinetics especially for inactivated virus vaccines, remain to be investigated.

In line with this, we analyzed immune dynamic up to 12 months using finger blood samples from four healthy young people immunized with following three-dose inactivation virus vaccination (Coronavac). Fig. 4 show the response dynamic curves of IgG-S detected by c-LOFI4, in which 4 negative samples and 48 positive samples, obtained before and after vaccination, respectively, were tested. Before vaccination, no anti-SARS-CoV-2 antibodies was detected for all finger blood samples. After a week of one-dose vaccination, the IgG-S was detected in all vaccination donors, indicating that the vaccine induced the humoral immune reaction. The higher IgG antibody concentration was obtained after two weeks and then decreased, which was similar with previous reports. At the 21st day, the second-dose vaccine of all donors was injected. Similarly, the IgG-S concentration of all donors rapidly increased and by far higher than that of first vaccine. The highest IgG-S concentration was 73 μg/mL. However, different with previous studies [34,36], the high concentration of IgG-S did not last a long time, but rapidly decreased and then reached a platform. Even through two hundred days later, the concentration of IgG-S kept a stabile value. After third-dose vaccine, a

higher IgG-S concentration were obtained in all donors, which was almost three times higher than those of the first-dose vaccine. Surprisedly, the IgG-S concentration also rapidly decreased and then reached a platform similar with that of the second vaccine. This decline in seropositivity over time might explain why an increase infection breakthrough was observed in cases among vaccinated individuals, even for third booster vaccine [36-38]. Even though our data provided humoral immune response for the observation of vaccination cohorts, a deeper investigation carried out by c-LOFI will be needed because of the limitation of the small sample size.

4 Conclusion

A portable and rapid detection platform (c-LOFI) was proposed for detection of anti-SARS-CoV-2 antibodies, which can meet the growing demand for extensive antibody testing facing with the ongoing pandemic and the population-wide vaccine deployment. The c-LOFI can quantitatively detects IgG-S or IgM-S in whole blood with simple dilution using functional fiber bio-probe and their respective HRP labeled secondary antibodies. Using the c-LOFI, the IgG-S and IgM-S gave excellent linearity over the range of 1.8 ng/mL to 984.9 ng/mL and from 0.6 ng/mL to 23.7 ng/mL, and displayed an LOD of 0.6 ng/ mL and 0.3 ng/ mL for IgG and IgM antibody, respectively. The real-time simultaneous detection of IgG-S and IgM-S is helpful for the infection progression tracking. Furthermore, the longitudinal immune response kinetics following vaccination was analyzed based on the proposed method, which provided valuable information for diagnosis, treatment, vaccine research, epidemiological research for COVID-19.

AUTHOR CONTRIBUTION

Wenjuan Xu: Conceptualization, methodology, data curation, writing original draft, writing—review & editing. Dang Song: Methodology, investigation, writing—review & editing. Jiayao Liu: Methodology, investigation. Xiangzhi Han: Methodology. Jiaxin Xu: Methodology. Anna Zhu: Conceptualization, supervision, writing—review & editing. Feng Long: Conceptualization, methodology, funding acquisition, project administration, supervision, writing—original draft, writing—review & editing.

ACNOWLEDGMENTS

This study was supported by the National Natural Science Foundation of China (Grant No. 21675171).

CONFLICT OF INTEREST

The authors declare no conflict of interest.

DATA AVAILABILITY STATEMENT

The data that supports the findings of this study are available in the supplementary material of this article.

References

1. Zhu N, Zhang D, Wang W, et al. A Novel Coronavirus from Patients with Pneumonia in China, 2019. *N Engl J Med* 2020; 382(8):727-733.

2. Cromer D, Juno JA, Khoury D, et al. Prospects for durable immune control of SARS-CoV-2 and prevention of reinfection. *Nat Rev Immunol* 2021; 21(6): 395-404.

3. Wang H, Yuan Y, Xiao M, et al. Dynamics of the SARS-CoV-2 antibody response up to 10 months after infection. *Cell Mol Immunol* 2021; 18:1832-1834.

4. Kaku CI, Champney ER, Normark J, et al. Broad anti-SARS-CoV-2 antibody immunity induced by heterologous ChAdOx1/mRNA-1273 vaccination. *Science (80-)* 2022; 375(6584):1041-1047.

5. WHO. Statement on the meeting of the International Health Regulations (2005) Emergency Committee regarding the outbreak of novel coronavirus (2019-nCoV). *WHO Newsl* 2020.

6. van Doremalen N, Bushmaker T, Morris DH, et al. Aerosol and Surface Stability of SARS-CoV-2 as Compared with SARS-CoV-1. *N Engl J Med* 2020; 382(16): 1564-1567.

7. Thompson D, Lei Y. Mini Review: Recent progress in RT-LAMP enabled COVID-19 detection. *Sensors and Actuators Reports* 2020; 2(1):100017.

8. Kotaki R, Adachi Y, Moriyama S, et al. SARS-CoV-2 Omicron-neutralizing memory B cells are elicited by two doses of BNT162b2 mRNA vaccine. *Sci Immunol* 2022; 7(70):eabn8590.

9. Ong SWX, Tan YK, Chia PY, et al. Air, Surface Environmental, and Personal Protective Equipment Contamination by Severe Acute Respiratory Syndrome Coronavirus 2 (SARS-CoV-2) from a Symptomatic Patient. *JAMA - J Am Med Assoc* 2020; 323(16):1610-1612.

10. Harvey WT, Carabelli AM, Jackson B, et al. SARS-CoV-2 variants, spike mutations and immune escape. *Nat Rev Microbiol* 2021; 19:409-424.

11. Qin Z, Peng R, Baravik IK, Liu X. Fighting COVID-19: Integrated Micro- and Nanosystems for Viral Infection Diagnostics. *Matter* 2020; 3(3):628-651.

12. Han Y, Duan X, Yang L, et al. Identification of SARS-CoV-2 inhibitors using lung and colonic organoids. *Nature* 2021; 589:270-275.

13. Wang W, Xu Y, Gao R, et al. Detection of SARS-CoV-2 in Different Types of Clinical Specimens. *JAMA - J Am Med Assoc* 2020; 323(18): 1843-1844.

14. Sidiq Z, Hanif M, Dwivedi KK, Chopra KK. Benefits and limitations of serological assays in COVID-19 infection. *Indian J Tuberc* 2020; 67(4):S163-S166.

15. Wu JL, Tseng WP, Lin CH, et al. Four point-of-care lateral flow immunoassays for diagnosis of COVID-19 and for assessing dynamics of antibody responses to SARS-CoV-2. *J Infect* 2020; 81(3):435-442.

16. Grifoni A, Sidney J, Zhang Y, Scheuermann RH, Peters B, Sette A. A Sequence Homology and Bioinformatic Approach Can Predict Candidate Targets for Immune Responses to SARS-CoV-2. *Cell Host Microbe* 2020; 27(4):671-680.

17. Li Z, Yi Y, Luo X, et al. Development and clinical application of a rapid IgM-IgG combined antibody test for SARS-CoV-2 infection diagnosis. *J Med Virol* 2020; 92(9): 1518-1524.

18. Yokoyama R, Kurano M, Morita Y, et al. Validation of a new automated chemiluminescent anti-SARS-CoV-2 IgM and IgG antibody assay system detecting both N and S proteins in Japan. *PLoS One* 2021; 16:e0247711.

19. Morales-Narváez E, Dincer C. The impact of biosensing in a pandemic outbreak: COVID-19. *Biosens Bioelectron* 2020; 163:112274.

20. Robosa RS, Sandaradura I, Dwyer DE, O'Sullivan MVN. Clinical evaluation of SARS-CoV-2 point-of-care antibody tests. *Pathology* 2020; 52(7):783-789.

21. Long QX, Tang XJ, Shi QL, et al. Clinical and immunological assessment of asymptomatic SARS-CoV-2 infections. *Nat Med* 2020; 26:1200-1204.

22. Vaiano P, Carotenuto B, Pisco M, et al. Lab on Fiber Technology for biological sensing applications. *Laser Photonics Rev* 2016; 6:922-961.

23. Ricciardi A, Crescitelli A, Vaiano P, et al. Lab-on-fiber technology: A new vision for chemical and biological sensing. *Analyst* 2015; 140:8068-8079.

24. Principe S, Giaquinto M, Micco A, et al. Thermo-plasmonic lab-on-fiber optrodes. *Opt Laser Technol* 2020; 132:106502.

25. Kanji JN, Bailey A, Fenton J, et al. Stability of SARS-CoV-2 IgG in multiple laboratory conditions and blood sample types. *J Clin Virol* 2021; 142:104933.

26. Zeng L, Li Y, Liu J, et al. Rapid, ultrasensitive and highly specific biosensor for the diagnosis of SARS-CoV-2 in clinical blood samples. *Mater Chem Front* 2020; 7:2000-2005.

27. Vasylieva N, Ahn KC, Barnych B, Gee SJ, Hammock BD. Development of an Immunoassay for the Detection of the Phenylpyrazole Insecticide Fipronil. *Environ Sci Technol* 2015; 49:10038-10047.

28. Cui X, Vasylieva N, Wu P, et al. Development of an Indirect Competitive Enzyme-Linked Immunosorbent Assay for Glycocholic Acid Based on Chicken Single-Chain Variable Fragment Antibodies. *Anal Chem* 2017; 89(20):11091-11097.

29. Liu H, Dai E, Xiao R, et al. Development of a SERS-based lateral flow immunoassay for rapid and ultra-sensitive detection of anti-SARS-CoV-2 IgM/IgG in clinical samples. *Sensors Actuators, B Chem* 2021; 329:129196.

30. Wang C, Yang X, Gu B, et al. Sensitive and Simultaneous Detection of SARS-CoV-2-Specific IgM/IgG Using Lateral Flow Immunoassay Based on Dual-Mode Quantum Dot Nanobeads. *Anal Chem* 2020; 92(23):15542-15549.

31. Hu F, Shang X, Chen M, Zhang C. Joint Detection of Serum IgM/IgG Antibody Is an Important Key to Clinical Diagnosis of SARS-CoV-2 Infection. *Can J Infect Dis Med Microbiol* 2020; 1020843.

32. Mccance K, Wise H, Simpson J, et al. Evaluation of SARS-CoV-2 antibody point of care devices in the laboratory and clinical setting. *Plos One*. doi: 10.1371/journal.pone.0266086.

33. Bauer G. The potential significance of high avidity immunoglobulin G (IgG) for protective immunity towards SARS-CoV-2. *Int J Infect Dis* 2021; 106:61-64.

34. Jiang XL, Wang GL, Zhao XN, et al. Lasting antibody and T cell responses to SARS-CoV-2 in COVID-19 patients three months after infection. *Nat Commun* 2021; 12(1):897.

35. Song D, Liu J, Xu W, et al. Rapid and quantitative detection of SARS-CoV-2 IgG antibody in serum using optofluidic point-of-care testing fluorescence biosensor. *Talanta* 2021; 235:122800.

36. Evans JP, Zeng C, Carlin C, et al. Neutralizing antibody responses elicited by SARS-CoV-2 mRNA vaccination wane over time and are boosted by breakthrough infection. *Sci Transl Med* 2022; 14(637):eabn8057.

37. Farinholt T, Doddapaneni H, Qin X, et al. Transmission event of SARS-CoV-2 delta variant reveals multiple vaccine breakthrough infections. *BMC Med* 2021; 19(1).

38. Nowroozi A, Rezaei N. Severe acute respiratory coronavirus virus 2 (SARS-CoV-2) delta variant of concern breakthrough infections: Are vaccines failing us? *Infect Control Hosp Epidemiol* 2021; 6:1-2.

Figures

Scheme 1. Design of c-LOFI and detection mechanism of anti-SARS-CoV-2 antibodies. (A) Schematic of the c-LOFI consisting of microfluidic system, optical system, signal treatment and control system, and mini-computer. (B) Detection mechanism of IgG-S based on chemiluminescent sandwich immunoassay principle.

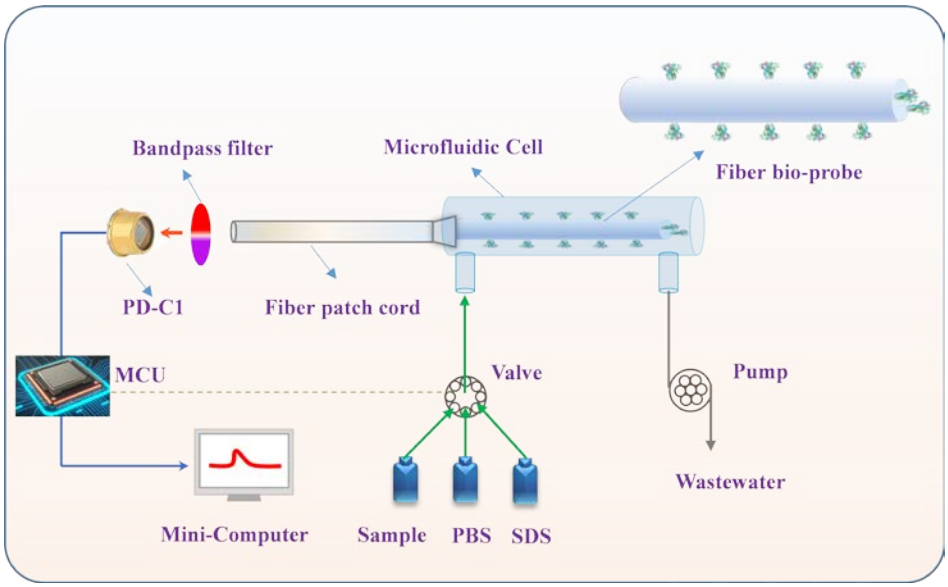

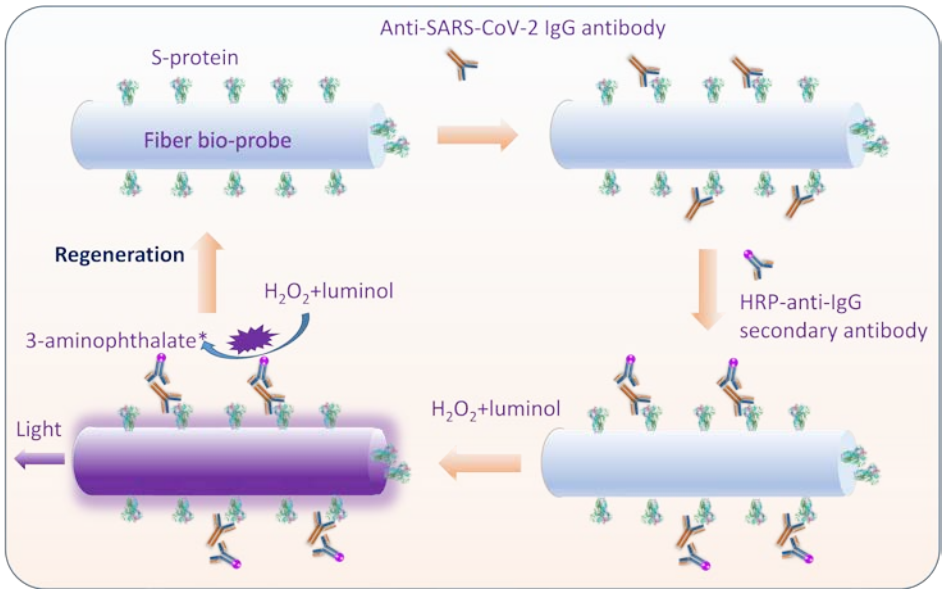

Figure 1. Characterization of S-protein functionalized bio-probe and c-LOFI. (A) Typical detection process and signal curve for IgG-S antibody detection. 5.0 μg/mL IgG-S and 0.5 μg/mL HRP labeled anti-IgG secondary antibody. (B) Typical detection process and signal curve for IgM-S detection. 100 ng/mL IgM-S and 1.0 μg/mL HRP labeled anti-IgM secondary antibody. (C) Verification of the CL signal came from binding reaction between antibody and antigen. (a) CL substrate solution was directly added; (b) 0.5 μg/mL HRP labeled anti-IgG secondary antibody and CL substrate solution was sequentially added; (c) 1.0 μg/mL HRP labeled anti-IgM secondary antibody and CL substrate solution was sequentially added; (d) 100 ng/mL IgM-S, 0.5 μg/mL HRP labeled anti-IgG secondary antibody, and CL substrate solution was sequentially added; (e) 5.0 μg/mL IgG-S, 1.0 μg/mL HRP labeled anti-IgM secondary antibody, and CL substrate solution was sequentially added; (f) 5.0 μg/mL IgG-S, 0.5 μg/mL HRP labeled anti-IgG secondary antibody, and CL substrate solution was sequentially added; (g) 100 ng/mL IgM-S, 1.0 μg/mL HRP labeled anti-IgM secondary antibody, and CL substrate solution was sequentially added. (D) Images of confocal fluorescence microscope for S-protein functionalized bio-probe (a), only addition of Cy5.5 labeled anti-IgG secondary antibody (b), and sequential addition of IgG-S and Cy5.5 labeled anti-IgG secondary antibody (c). (E) Specificity of the S-protein functionalized fiber bio-probe, and the concentration of anti-MERS-CoV antibody, anti-HCoV-HKU1 antibody, and normal Human IgG is 100 ng/mL, 100 ng/mL IgM-S, 1.0 μg/mL HRP labeled anti-IgM secondary antibody. The error bars were the standard deviation of three repeated experiments (n=3).

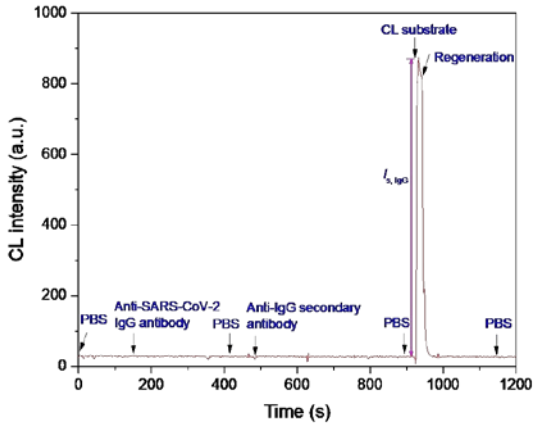

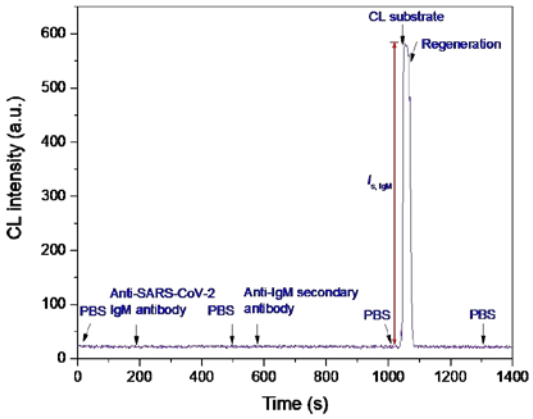

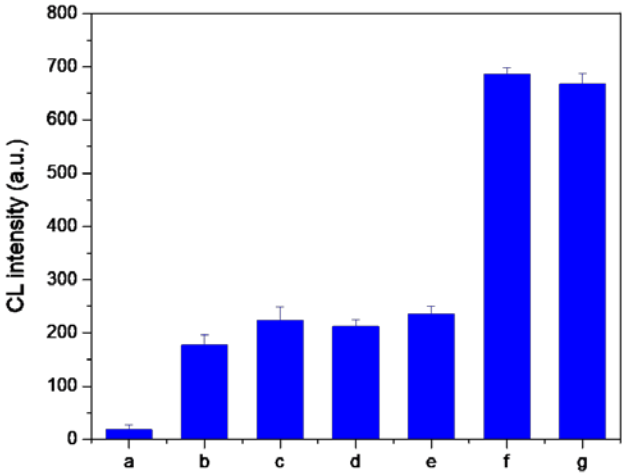

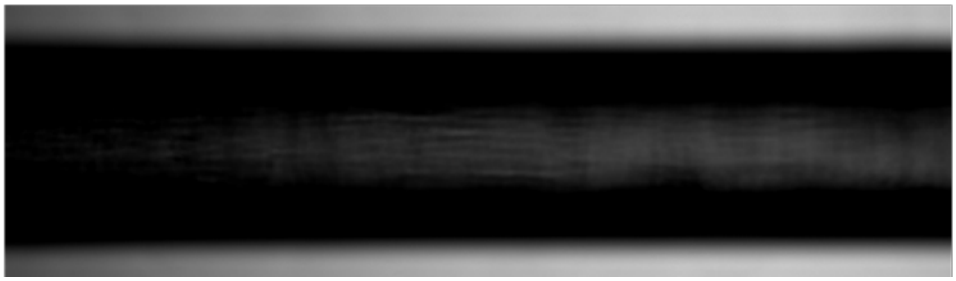

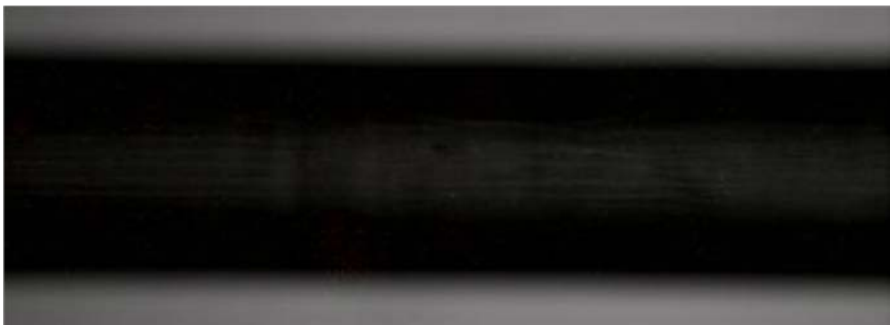

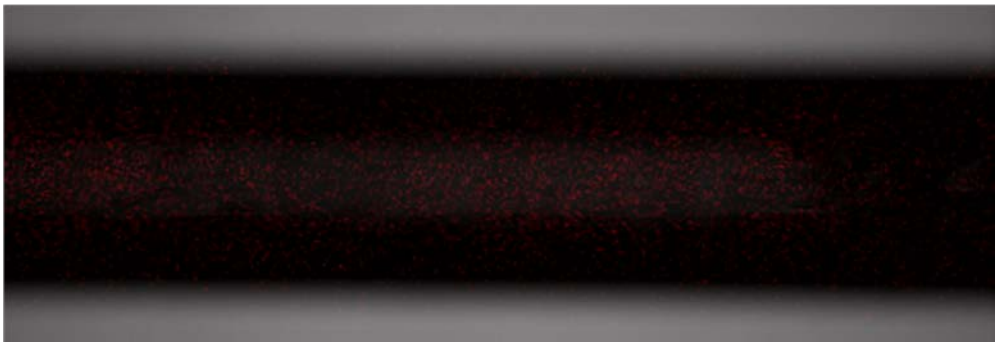

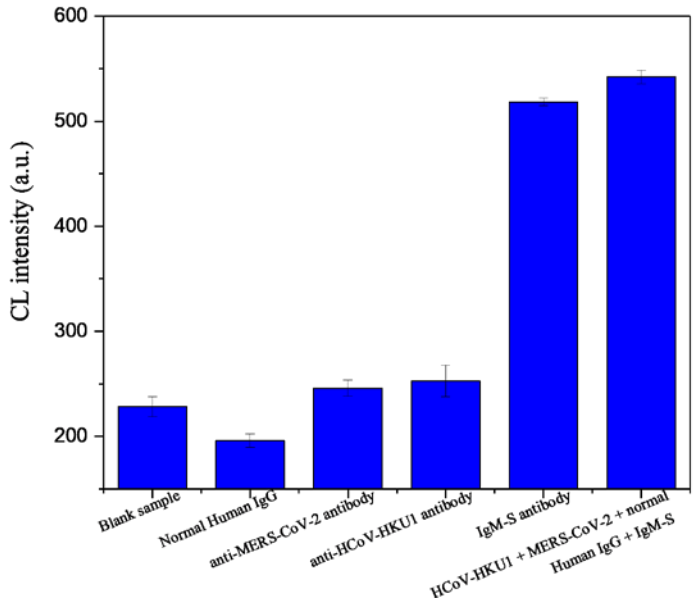

Figure 2. Typical signal curves of (A) IgM-S detection and (B) IgG-S detection using the c-LOFI; (C) Dose-response curve of IgM-S detection (1.0 μg/mL HRP-labeled anti-IgM secondary antibody); (D) Dose-response curve of IgG-S detection (0.5 μg/mL HRP-labeled anti-IgG secondary antibody) (n=3).

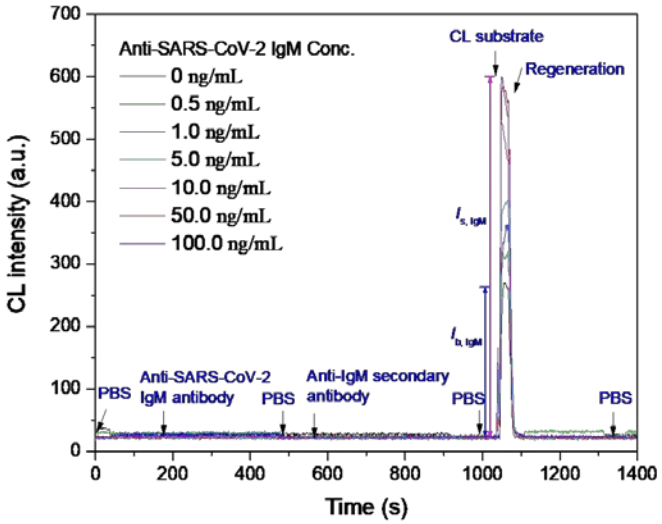

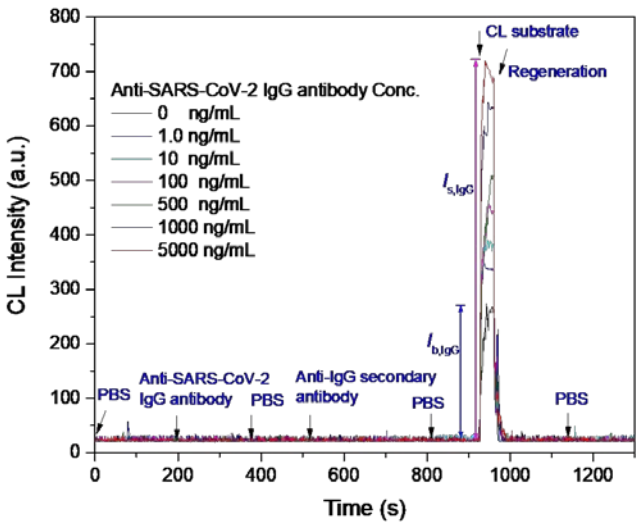

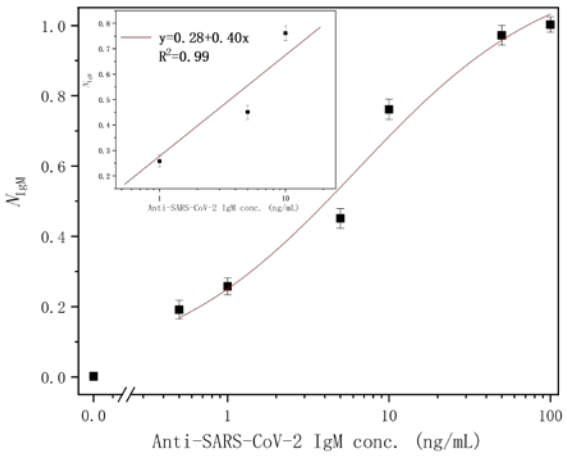

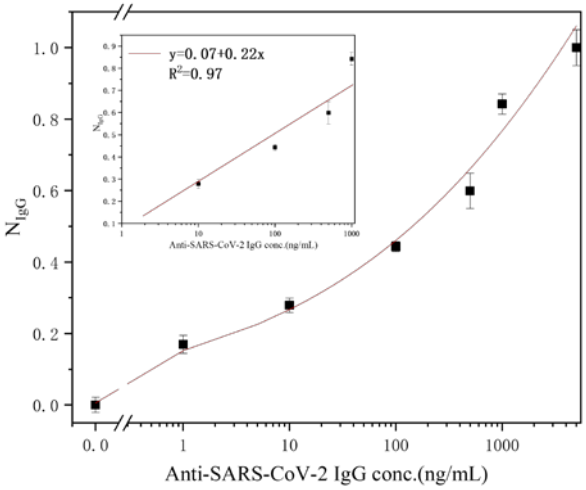

Figure 3. Typical signal curves of (A) IgM-S detection and (B) IgG-S detection using c-LOFI system in blood; (C) dose-response curve of IgM-S detection in blood (1.0 μg/mL secondary antibody); (D) dose-response curve of IgG-S detection in blood (0.5 μg/mL secondary antibody) (n=3).

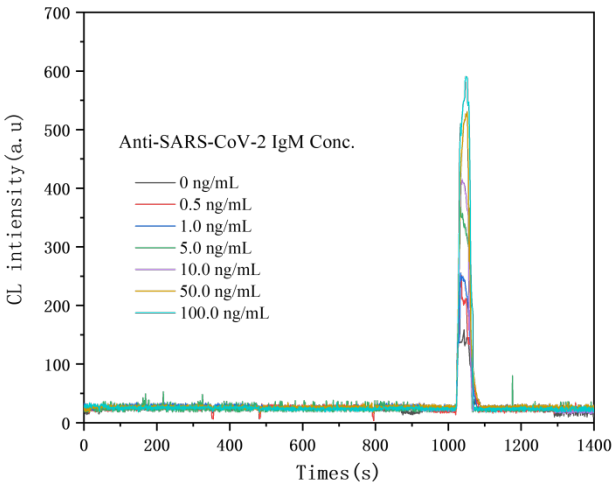

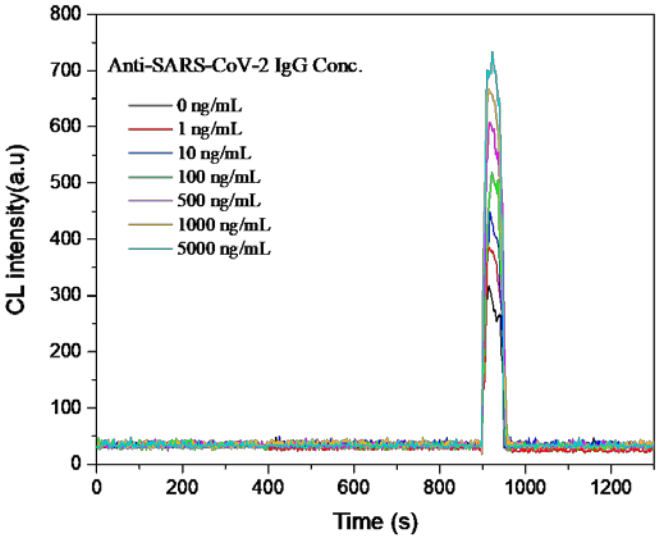

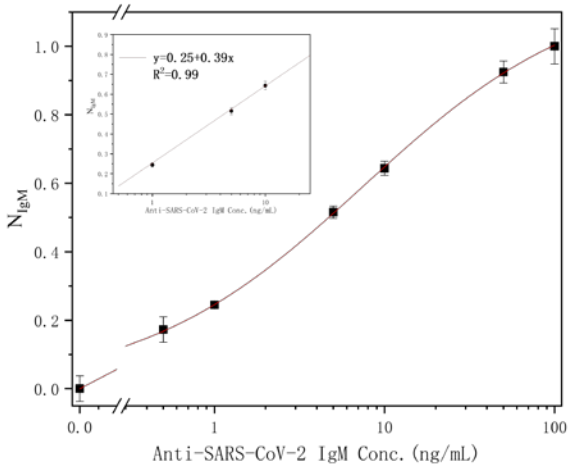

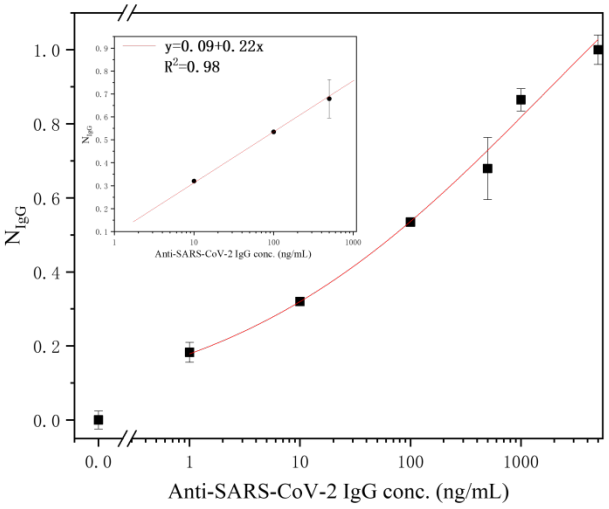

Figure 4. Immune response kinetics with three-dose inactivation virus vaccination. 4 negative samples and 48 positive samples, obtained before and after vaccination, respectively, were tested.